Radio-over-fiber transmission from an optically injected semiconductor laser in period-one state

Sze-Chun Chan*[a], Sheng-Kwang Hwang[b], Jia-Ming Liu[a]
[a]Electrical Engineering Department, University of California, Los Angeles, California 90095-1594;
[b]Graduate Institute of Opto-Mechatronics, National Chung Cheng University, Chia-Yi 621, Taiwan

ABSTRACT

Nonlinear dynamics of semiconductor lasers has found many interesting applications in microwave photonics technology. In particular, a semiconductor laser under optical injection of proper strength and optical frequency detuning can enter into the dynamical period-one (P1) state through Hopf bifurcation. The resulting optical output carries a broadly tunable high-speed microwave modulation without employing any expensive microwave electronics. It is therefore a desirable source for radio-over-fiber (RoF) applications. The P1 state can also be adjusted to have a nearly single sideband (SSB) optical spectrum. It is an advantageous property for long distance fiber transmission because it minimizes the microwave power penalty that is induced by chromatic dispersion. In this work, we investigate in detail the properties of the P1 state and the effect of fiber dispersion as a function of the injection conditions. Based on a well-established rate equation model, the results show that the generated microwave frequency can be several times higher than the intrinsic relaxation resonance frequency of the laser. With a large injection strength and an injection detuning frequency higher than that required for Hopf bifurcation, the generated microwave power is nearly constant and the optical spectrum is close to SSB. We simulate the effect of fiber chromatic dispersion and the result shows a maximum microwave power penalty of less than 2 dB. The characterization of the P1 state is useful in guiding the design of RoF systems based on optically injected semiconductor lasers.

Keywords: Optical injection, semiconductor laser, microwave photonics, radio-over-fiber, single sideband.

1. INTRODUCTION

Radio-over-fiber (RoF) technology has recently attracted much attention.[1-6] In an RoF system, microwave signal is carried on an optical wave that is transmitted through optical fibers. It enables microwave transmission over very long distances. The technology greatly simplifies the hardware design in wireless communication networks. For instance, it is used to implement low-cost photonic microwave links between the central office and remote base stations.

Despite its many advantages, RoF systems are often hindered by the microwave power penalty caused by chromatic dispersion. The problem can only be circumvented by using the single-sideband (SSB) modulation scheme. As a result, different SSB sources are developed such as using two-laser heterodyning,[6] SSB electro-optic modulators,[7] external cavity semiconductor lasers,[8] optical filtering techniques,[9] and multi-section semiconductor lasers.[5] However, these methods are usually limited in terms of microwave stability, optical efficiency, or frequency tunability.

In this paper, we report on an RoF source based on an optically injected semiconductor laser.[2-3] The injection invokes the intrinsic nonlinear dynamics of the laser into the period-one oscillation state. The oscillation causes a microwave modulation on the optical carrier. The system therefore becomes a photonic microwave source.[10-13] This source is widely tunable far beyond the original modulation bandwidth of the laser. It requires no lossy external modulation optics. The photonic microwave can also be stabilized using simple several microwave locking methods. By properly adjusting the injection conditions, the modulation can become nearly SSB to eliminate the chromatic dispersion-induced power penalty. Experimentally, we demonstrate a 40-GHz photonic generation that is stabilized by subharmonic microwave locking. Numerically, we investigate the power penalty performance of our RoF source. The results show that the optically injected semiconductor laser in the period-one state is an ideal candidate for RoF applications.

Following this introduction, the experiment and simulation are presented in Sections 2 and 3, respectively. They are followed by discussions in Section 4 and a conclusion in Section 5.

*scchan@ucla.edu; phone 1-310-825-8650

Physics and Simulation of Optoelectronic Devices XV, edited by Marek Osinski, Fritz Henneberger, Yasuhiko Arakawa,
Proc. of SPIE Vol. 6468, 646811, (2007) · 0277-786X/07/$18 · doi: 10.1117/12.699170

2. EXPERIMENT

The experimental setup of the optical injection system is shown in Fig. 1. The lasers used are 1.3-μm single-mode distributed feedback (DFB) semiconductor lasers (Bookham Technology LC131). The master laser (ML) is biased at 106.2 mA, which is 7.08 times its threshold, and is temperature stabilized at 15.90 °C. The slave laser (SL) is biased at 40.0 mA, which is 2.22 times its threshold, and is temperature stabilized at 18.00 °C. It emits an optical power of about 4.5 mW and has a relaxation resonance frequency at around 10 GHz. Light from the master laser is directed by the mirror (M) and the beam splitter (BS) into the slave laser. About 7 mW of optical injection power impinges on the front facet of the slave laser, but only a small portion is successfully coupled into the mode of the slave laser cavity. Feedback from the slave laser to the master laser is prevented by the optical isolator (OI). Under the above bias currents, the optical frequency of the master laser is detuned from the free-running optical frequency of the slave laser by f_i = +30.7 GHz. The injection drives the slave laser into period-one oscillation with a fundamental frequency of f_0 = 40 GHz. The light from the slave laser is transmitted through an optical fiber (F). The optical spectrum is monitored by an optical spectrum analyzer (OSA) (Newport SR-260-C). The power spectrum is monitored by a power spectrum analyzer (PSA) (Agilent 8565EC) after detection by a 45-GHz photodiode (PD) (New Focus 1011). A microwave frequency synthesizer (MFS) (HP 83620A) can be used to apply a current modulation onto the slave laser.

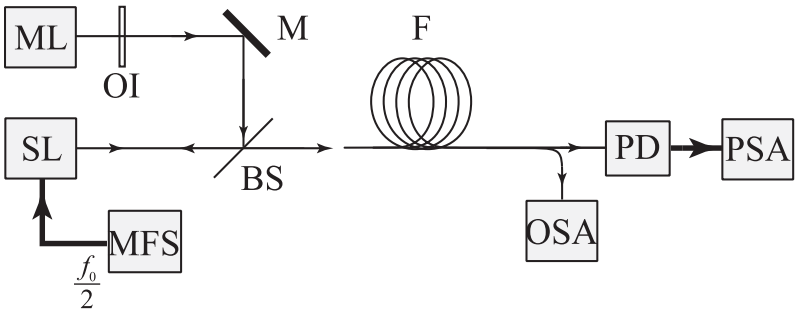

Fig. 1. Schematics of the experimental setup. ML: master laser; SL: slave laser; OI: optical isolator; M: mirror; BS: beam splitter; F: fiber; PD: photodiode; PSA: power spectrum analyzer; OSA: optical spectrum analyzer; and MFS: microwave frequency synthesizer. Thin and thick lines correspond to optical and microwave paths, respectively.

Figure 2 shows the spectra obtained as the slave laser is operated in period-one oscillation. The optical spectrum in Fig. 2(a) is offset to the free-running frequency of the slave laser. Unlike a free-running laser that emits only a single line at the zero offset, the optically injected slave laser emits two lines of approximately equal magnitudes. The line at f_i = 30.7 GHz offset is due to the injection from the master laser, whereas the line at $f_i - f_0 = -9.3$ GHz is due to the period-one oscillation at f_0 = 40 GHz. The beating of the two lines results in the power spectrum as shown in Fig. 2(b). The signal is very noisy because of the intrinsic fluctuations of the system, such as the spontaneous emission noise of the slave laser and the power variation from the master laser injection.

In order to improve the signal purity, we apply a stable current modulation to lock the period-one oscillation. In this experiment, we demonstrate subharmonic microwave locking by applying an external microwave at $f_0/2$ to lock the fundamental at f_0.[14] With a modest modulation strength of 5 dBm, the signal can be drastically improved. The stabilized signal is shown in Fig. 2(c) at a much reduced span. Compared to the direct locking method using an external source at f_0,[13] the subharmonic locking technique allows us to use an external source at a reduced frequency. It is particularly useful for generating high frequency microwave beyond the usual bandwidth of electronic components.

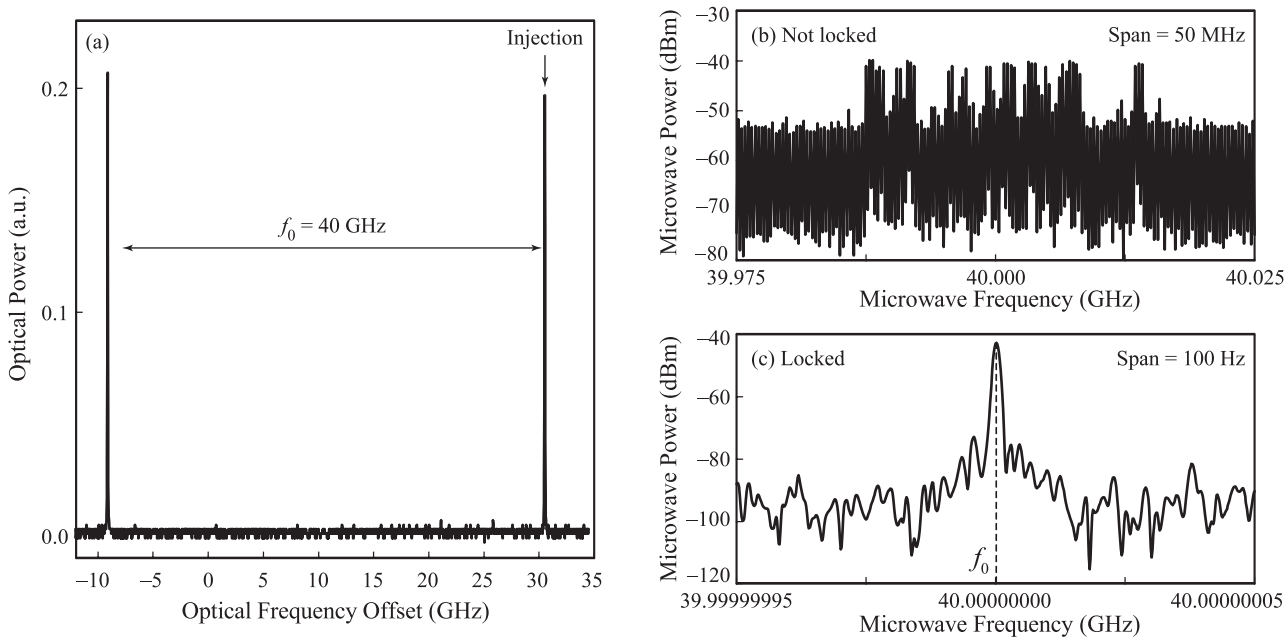

Fig. 2. Experimental spectra of the slave laser under period-one oscillation at f_0 = 40 GHz. The optical injection is 7 mW at the input facet of the slave laser. It is detuned at f_i = +30.7 GHz above the free-running frequency of the slave laser. (a) Optical spectrum offset to the free-running frequency of the slave laser. (b) Power spectrum revealing the fluctuation between the two optical lines. (c) Power spectrum stabilized by current modulation at the subharmonic frequency $f_0/2$.

3. SIMULATION

The period-one state can be more extensively investigated through numerical simulation. We apply the well known rate equation model of the optical injection system as follows:[15]

$$\frac{\mathrm{d}a_\mathrm{r}}{\mathrm{d}t} = \frac{1}{2}\left[\frac{\gamma_\mathrm{c}\gamma_\mathrm{n}}{\gamma_\mathrm{s}\tilde{J}}\tilde{n} - \gamma_\mathrm{p}(a_\mathrm{r}^{\,2} + a_\mathrm{i}^{\,2} - 1)\right](a_\mathrm{r} + ba_\mathrm{i}) + \xi_\mathrm{i}\gamma_\mathrm{c}\cos 2\pi f_\mathrm{i} t \tag{1}$$

$$\frac{\mathrm{d}a_\mathrm{i}}{\mathrm{d}t} = \frac{1}{2}\left[\frac{\gamma_\mathrm{c}\gamma_\mathrm{n}}{\gamma_\mathrm{s}\tilde{J}}\tilde{n} - \gamma_\mathrm{p}(a_\mathrm{r}^{\,2} + a_\mathrm{i}^{\,2} - 1)\right](-ba_\mathrm{r} + \mathrm{i}a_\mathrm{i}) - \xi_\mathrm{i}\gamma_\mathrm{c}\sin 2\pi f_\mathrm{i} t \tag{2}$$

$$\frac{\mathrm{d}\tilde{n}}{\mathrm{d}t} = -\left[\gamma_\mathrm{s} + \gamma_\mathrm{n}(a_\mathrm{r}^{\,2} + a_\mathrm{i}^{\,2})\right]\tilde{n} - \gamma_\mathrm{s}\tilde{J}(a_\mathrm{r}^{\,2} + a_\mathrm{i}^{\,2} - 1) + \frac{\gamma_\mathrm{s}\gamma_\mathrm{p}}{\gamma_\mathrm{c}}\tilde{J}(a_\mathrm{r}^{\,2} + a_\mathrm{i}^{\,2})(a_\mathrm{r}^{\,2} + a_\mathrm{i}^{\,2} - 1) \tag{3}$$

where a_r and a_i respectively are the real and imaginary parts of normalized complex intracavity field amplitude at the free-running slave laser frequency, $1 + \tilde{n}$ is the normalized charge carrier density, $\tilde{J}$ is the normalized bias current above the threshold, ξ_i is the dimensionless injection strength, f_i is the injection detuning as before, γ_c is the cavity decay rate, γ_s is the spontaneous carrier relaxation rate, γ_n is the differential carrier relaxation rate, γ_p is the nonlinear carrier relaxation rate, and b is the linewidth enhancement factor. The following parameter values are adopted: γ_c = $5.36\times10^{11}(\mathrm{s}^{-1})$, γ_s = $5.96\times10^{9}(\mathrm{s}^{-1})$, γ_n = $7.53\times10^{9}(\mathrm{s}^{-1})$, γ_p = 2.34×10^{10} (s^{-1}), b = 3.2, and $\tilde{J}$ = 1.222. These fall within the ranges of the typical semiconductor laser parameters.[16-17] The relaxation resonance frequency is given by f_r = $(2\pi)^{-1}(\gamma_\mathrm{c}\,\gamma_\mathrm{n} + \gamma_\mathrm{s}\,\gamma_\mathrm{p})^{1/2} \approx$ 10 GHz. We conduct a second-order Runge-Kutta integration for a duration longer than 1 μs. The injection strength ξ_i is varied between 0 and 0.4, while the frequency detuning f_i is varied between 0 and 35 GHz.

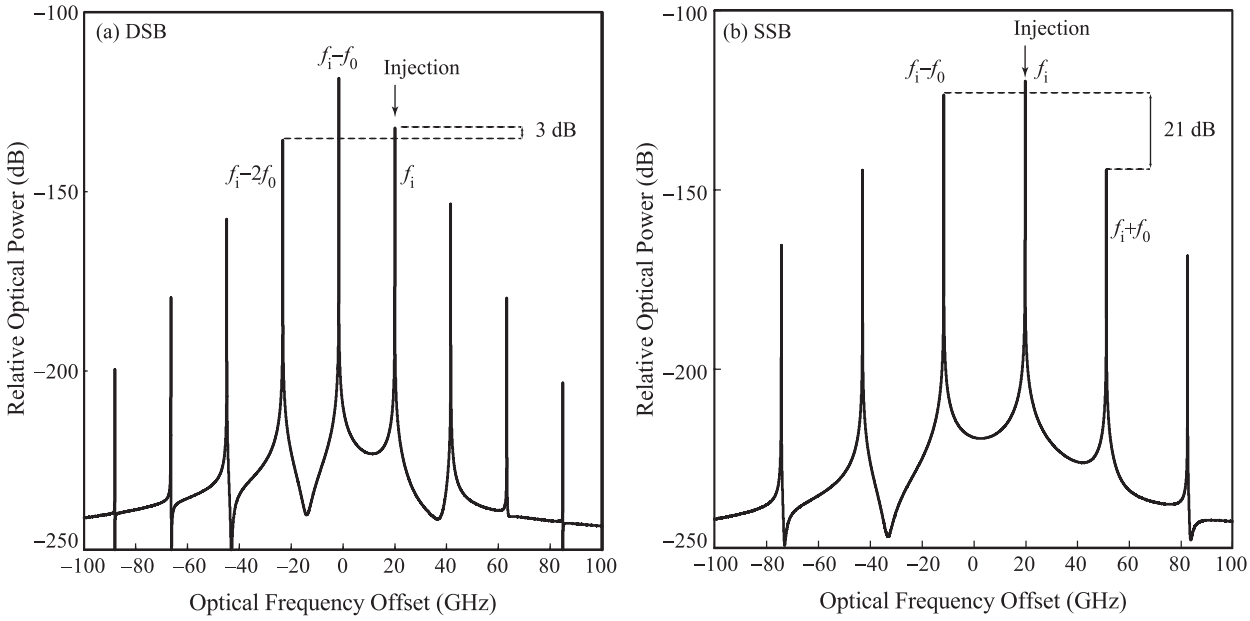

Fig. 3. Optical spectra of the slave laser in period-one states. (a) DSB period-one generated at $(\xi_i, f_i) = (0.065, 20\ \text{GHz})$. (b) SSB period-one generated at $(\xi_i, f_i) = (0.268, 20\ \text{GHz})$.

The optical spectra of two different period-one states are shown in Fig. 3. The detuning is kept constant at $f_i = 20$ GHz, but the injection strength ξ_i is varied. Both spectra consist of the regeneration of the injected light at f_i and many sideband separated by the period-one oscillation frequency f_0. However, the relative magnitudes of these frequency components changes with the injection strength. When $\xi_i = 0.065$ as in Fig. 3(a), the principal component is at $f_i - f_0$. It is surrounded by two sidebands at $f_i - 2f_0$ and f_i, which are of similar magnitudes. This period-one state is regarded as nearly double sideband (DSB) because the magnitude difference between the upper and lower sideband is only about 3 dB. On the other hand, when $\xi_i = 0.268$ as in Fig. 3(b), the principal component is at f_i, which corresponds to the injected light. It has two highly asymmetric sidebands. The lower sideband at $f_i - f_0$ is more than 21 dB stronger than the upper sideband at $f_i + f_0$. The period-one state is thus nearly SSB and is desirable for low power penalty RoF transmission. According to Fig. 3, we conclude that a period-one state can have an output of either DSB or SSB depending on the injection conditions. Therefore, the injection conditions need to be optimized for RoF transmission.

In order to illustrate the effect of chromatic dispersion on the microwave power, we simulate the fiber transmission of the photonic microwave generated by the period-one state. The dispersion coefficient is assumed to be 17 ps/km-nm, as in a typical single-mode fiber. At the receiving end, a photodiode is used to extract the optically carried microwave. We calculate the fundamental microwave power P_{f0} at f_0 and the second harmonic microwave power P_{2f0} at $2f_0$. The results are shown in Fig. 4 for the same DSB and SSB states considered previously in Fig. 3. For the DSB period-one state in Fig. 4(a), a repetitive and deep variation of the microwave power is observed as the fiber length increases. It is because the dispersive propagation changes the phase relation between the two sidebands. When the upper and the lower sidebands are in-phase, the optical signal corresponds to a pure amplitude modulation and it generates the maximum microwave power P_{f0}. When the sidebands are out-of-phase, the signal corresponds to an optical phase modulation and it cannot be detected by the photodiode. Referring to Fig. 3(a), we see that the microwave P_{f0} is generated from the beating of $f_i - f_0$ and f_i, and the beating of $f_i - f_0$ and $f_i - 2f_0$. Dispersion introduces a length-dependent phase between the beat signals, which causes the periodic power variation. The maximum power penalty of $\Delta P_{f0} = 16$ dB is observed in Fig. 4(a). By contrast, the SSB period-one state in Fig. 4(b) experiences only a small power variation of $\Delta P_{f0} = 2$ dB. The improvement is expected from the corresponding optical spectrum in Fig. 3(b). It is because the microwave power P_{f0} is generated predominately by the beating of $f_i - f_0$ and f_i only. There is no phase issue for the SSB case.

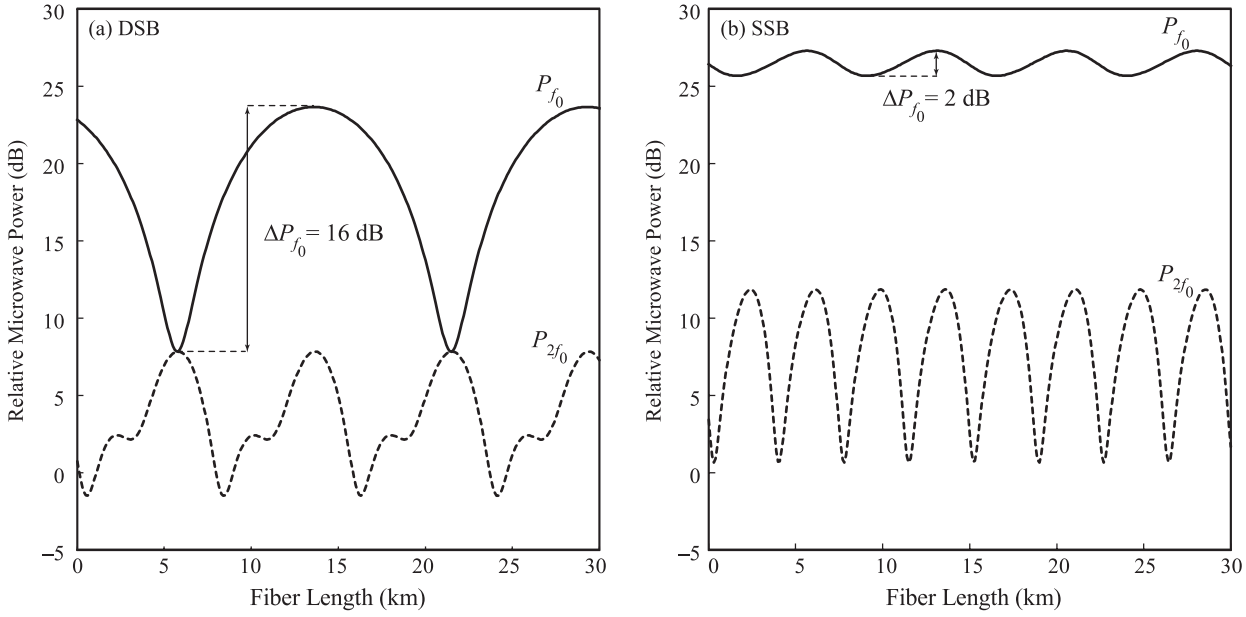

Fig. 4. Microwave power at the fundamental f_0 and the second-harmonic $2f_0$ received after propagation in fiber. (a) DSB period-one generated at (ξ_i, f_i) = (0.065, 20 GHz). (b) SSB period-one generated at (ξ_i, f_i) = (0.268, 20 GHz).

A more complete representation is shown in Fig. 5 as the mappings over the injection parameters ξ_i and f_i. In Fig. 5(a), the contours of the fundamental frequency of the period-one state are shown. A wide region of period-one oscillation is found above the well-studied Hopf bifurcation line, except for a confined region of chaotic states. Within the period-one region, the fundamental frequency f_0 generally increases with the both ξ_i and f_i. Frequencies of up to 4 times the relaxation resonance at 10 GHz can be obtained. Thus, the photonic microwave source is broadly tunable and is not limited by the conventional modulation bandwidth of the semiconductor laser

Figure 5(b) presents the power penalty performance as the maximum power variation ΔP_{f0} for an arbitrary fiber length. The region slightly above the Hopf bifurcation line is shown to be most immune to the power penalty. It corresponds to the region of SSB period-one states. Combining Figs. 5(a) and (b), we observe that the period-one state can be broadly tuned between f_0 = 22 and 42 GHz if a maximum power penalty of 3 dB can be tolerated. Therefore, the period-one state under properly adjusted injection is an ideal candidate for RoF applications that requires high immunity to power penalty.

4. DISCUSSION

The laser dynamical parameters are known to have significant effect on the nonlinear dynamics of the optical injection system.[17] In particular, the nonlinear carrier relaxation rate γ_p is known to have a stabilization effect on the system. A reduced γ_p can therefore widen the period-one region. As a result, we are interested in investigating the effect of γ_p on RoF transmission.

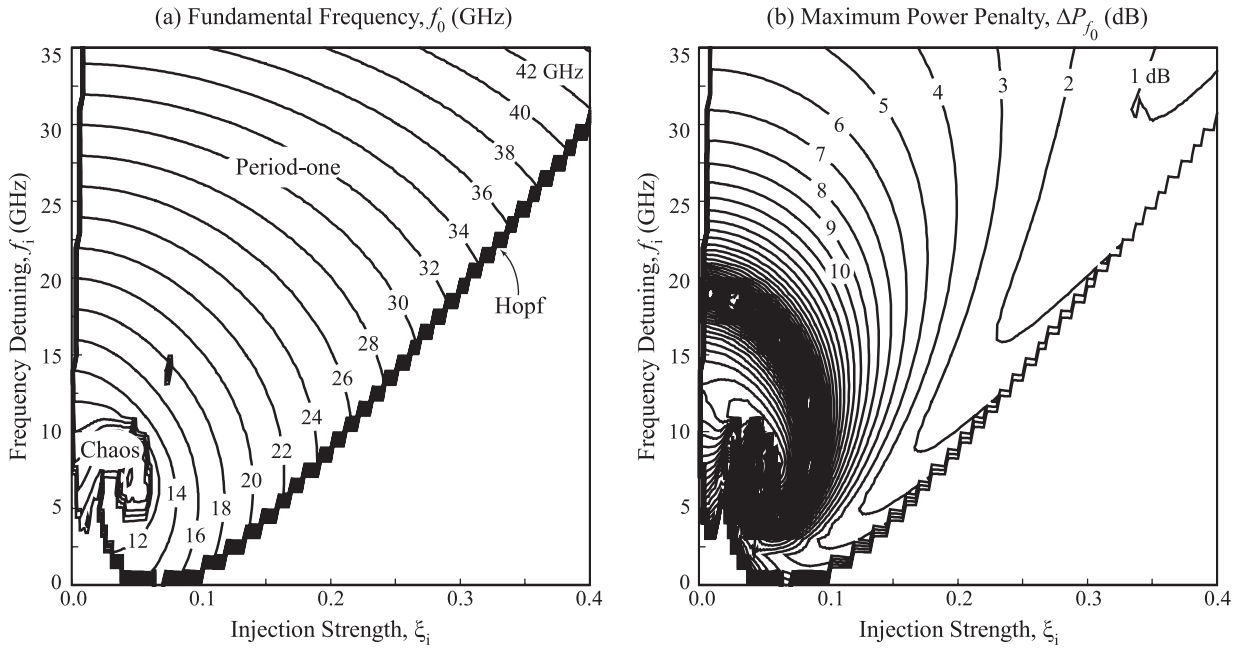

Fig. 5. Contour maps of (a) the fundamental period-one frequency f_0 and (b) the maximum power penalty ΔP_{f0} after fiber propagation.

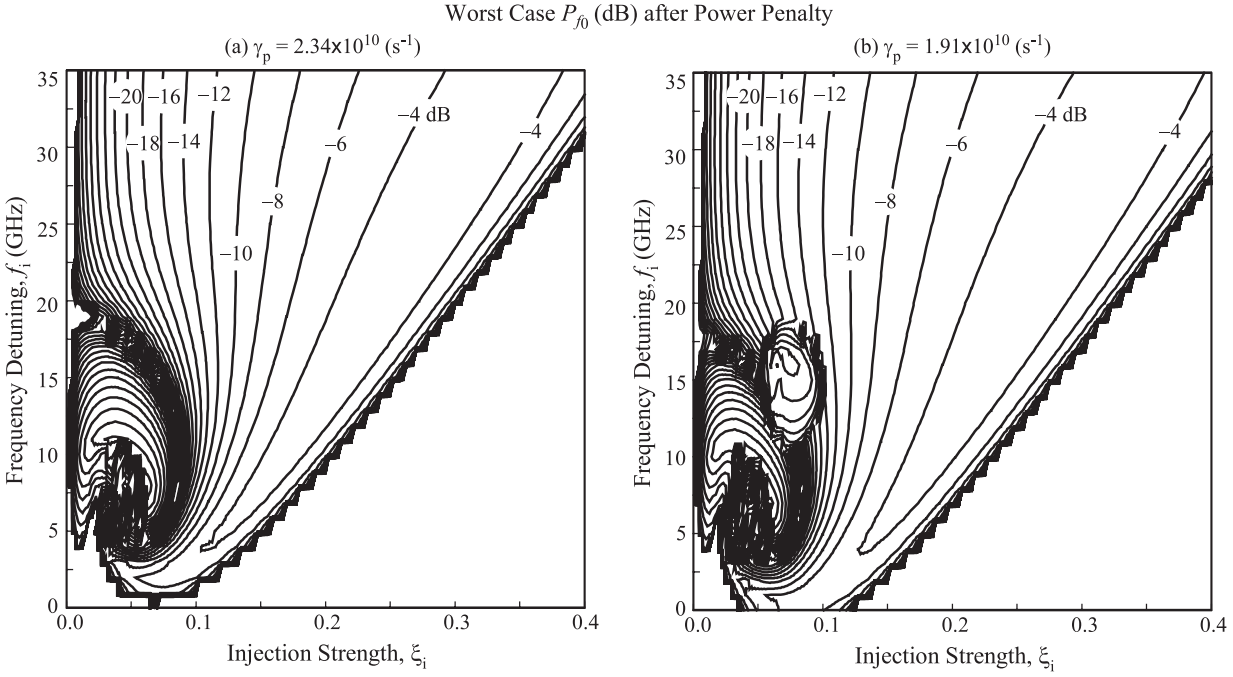

Fig. 6. Worst case microwave power received after propagation in a fiber, when (a) $\gamma_p = 2.34 \times 10^{10}$ (s^{-1}) and (b) $\gamma_p = 1.91 \times 10^{10}$ (s^{-1}).

For comparison, we analyze the worst case microwave power that can be guaranteed to the receiving end at an arbitrary distance away when the power penalty is considered. The mapping using the original γ_p is shown in Fig. 6(a), while that of a reduced γ_p is shown in Fig. 6(b). The mappings are normalized so that 0 dB corresponds to the highest microwave power that can be generated before the fiber propagation.

Figure 6 shows that the general structure of the mapping is maintained. The best region of operation is slightly above the Hopf bifurcation line, consistent with Fig. 5(b). The new γ_p is only slightly reduced by 18% from the original one, but its effect is observable as the enlargement of the period-one region shown in Fig. 6(b). The region of relatively high power is also widened, for example, the area enclosed by the −4-dB line is slightly broadened. Thus, reducing the value of γ_p increases the microwave power transmitted by the nonlinear period-one dynamics. These observations are consistent with the stabilization nature of γ_p.

5. CONCLUSION

RoF performance of an optically injected semiconductor laser under period-one oscillation is investigated. We experimentally demonstrate a 40-GHz photonic microwave generation incorporated with subharmonic microwave locking. We numerically simulate an optical injected laser under the period-one oscillation. Depending on the injection conditions, the spectrum of the oscillation can be DSB or SSB. The microwave power penalty induced by fiber chromatic dispersion is considered. When properly adjusted into SSB period-one oscillation, the system is shown to be quite immune to the power penalty. The system is least susceptible to the penalty when operated at the region slightly above the Hopf bifurcation line in the mapping. The results of this work illustrate that the optical injection system is suitable for low power penalty RoF transmission.

REFERENCES

1. L. A. Johansson and A. J. Seeds, "Generation and transmission of millimeter-wave data-modulated optical signals using an optical injection phase-lock loop," *J. Lightwave Technol.* 21, 511-520 (2003).
2. S. C. Chan, S. K. Hwang, and J. M. Liu, "Radio-over-fiber AM-to-FM upconversion using an optically injected semiconductor laser," *Opt. Lett.* 31, 2254-2256 (2006).
3. S. K. Hwang and D. H. Liang, "Effects of linewidth enhancement factor on period-one oscillations of optically injected semiconductor lasers," *Appl. Phys. Lett.* 89, 061120 (2006).
4. A. Kaszubowska, L. P. Barry, and P. Anandarajah, "Effects of intermodulation distortion on the performance of a hybrid radio/fiber system employing a self-pulsating laser diode transmitter," *IEEE Photon. Technol. Lett.* 15, 852-854 (2003).
5. C. Lim, D. Novak, A. Nirmalathas, and G. H. Smith, "Dispersion-induced power penalties in millimeter-wave signal transmission using multisection DBR semiconductor laser," *IEEE Trans. Microwave Theory Tech.* 49, 288-296 (2001).
6. U. Gliese, "Multi-functional fibre-optic microwave links," *Opt. And Quantum Electron.* 30, 1005-1019 (1998).
7. J. Han, B. J. Seo, Y. Han, B. Jalali, and H. R. Fetterman, "Reduction of fiber chromatic dispersion effects in fiber-wireless and photonic time-stretching system using polymer modulators," *J. Lightwave Technol.* 21, 1504-1509 (2003).
8. K. S. Lee and C. Shu, "Stable and widely tunable dual-wavelength continuous-wave operation of a semiconductor laser in a novel Fabry-Perot grating-lens external cavity," *IEEE J. Quantum Electron.* 33, 1832-1838 (1997).
9. H. S. Ryu, Y. K. Seo, and W. Y. Choi, "Dispersion-tolerant transmission of 155-Mb/s data at 17 GHz using a 2.5-Gb/s-grade DFB laser with wavelength-selective gain from an FP laser diode," *IEEE Photon. Technol. Lett.* 16, 1942-1944 (2004).
10. S. K. Hwang, J. M. Liu, and J. K. White, "Characteristics of period-one oscillations in semiconductor lasers subject to optical injection," *IEEE J. Select. Topics Quantum Electron.* 10, 974-981 (2004).
11. S. C. Chan and J. M. Liu, "Tunable narrow-linewidth photonic microwave generation using semiconductor laser dynamics," *IEEE J. Select. Topics Quantum Electron.* 10, 1025-1032 (2004).
12. S. C. Chan and J. M. Liu, "Frequency modulation on single sideband using controlled dynamics of an optically injected semiconductor laser," *IEEE J. Quantum Electron.* 42, 699-705 (2006).
13. T. B. Simpson and F. Doft, "Double-locked laser diode for microwave photonics applications," *IEEE Photon. Technol. Lett.* 11, 1476-1478 (1999).

14. L. Noël, D. Wake, D. G. Moodie, D. D. Marcenac, L. D. Westbrook, and D. Nesset, "Novel techniques for high-capacity 60-GHz fiber-radio transmission systems," *IEEE Trans. Microwave Theory Tech.* 45, 1416-1423 (1997).
15. T. B. Simpson, J. M. Liu, K. F. Huang, and K. Tai, "Nonlinear dynamics induced by external optical injection in semiconductor lasers," *Quantum Semiclass. Opt.* 9, 765-784 (1997).
16. S. K. Hwang, J. M. Liu, and J. K. White, "35-GHz intrinsic bandwidth for direct modulation in 1.3-μm semiconductor lasers subject to strong injection locking," *IEEE Photon. Technol. Lett.* 16, 972-974 (2004).
17. S. K. Hwang and J. M. Liu, "Dynamical characteristics of an optically injected semiconductor laser," *Opt. Commun.* 183, 195-205 (2000).